

# Evaluation of Water Diffusion Confined in Epoxies: Role of Atomic Local Mobility of Polymer Chains

Yasuyuki Nakamura,\* Yuji Higuchi, Yoshihisa Fujii, and Masanobu Naito

Cite This: <https://doi.org/10.1021/acsapm.4c04089>

Read Online

ACCESS |

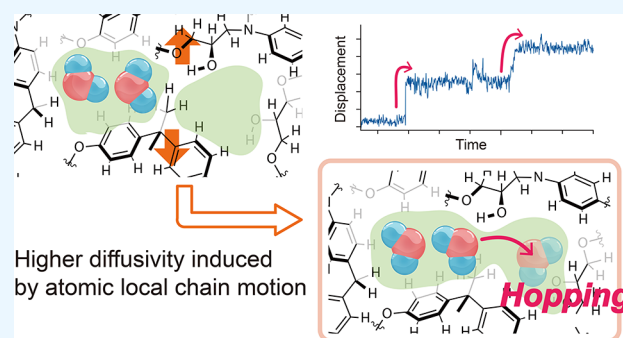
Metrics &amp; More

Article Recommendations

Supporting Information

**ABSTRACT:** The diffusion of water in epoxy resins is a fundamental property that characterizes their applications. While various factors influencing molecular diffusion in epoxies, such as voids and hydrogen bonding, have been widely investigated, the impact of chain mobility remains unclear. The dynamics of internal water molecules in two epoxy compositions with varying ratios were examined by molecular dynamics simulations, along with the relationship to the epoxy polymer chain mobility. The relationship between the characteristic hopping behavior of water molecules and epoxy polymer chain local mobility was explored by evaluating the atomic displacement of chain atoms over a short period, which is a distinctly smaller structural unit compared to segmental chain motion. This analysis showed a trend of high diffusivity of water molecules with high chain local mobility, with stoichiometric epoxy exhibiting higher values compared to epoxide-excess nonstoichiometric epoxy, which agrees with the experimental observations in QENS measurements. Atomic displacement, as the metric of chain local motion, illustrated that the discontinuous hopping behavior of water molecules occurs at locations of high chain local mobility, which leads to the transient interconnection of isolated voids in epoxy. This work suggests that water diffusivity is strongly related to chain local mobility in cross-linked resins because of the restriction of large-scale or segmental chain motion. This contributes to a better understanding of water-related properties in epoxy materials and facilitates the optimization of epoxy chemical structures.

**KEYWORDS:** epoxy, water, diffusion, mechanism, molecular dynamics simulations, chain motion



## INTRODUCTION

Epoxy resins are renowned for their excellent water resistance, establishing themselves as key polymer materials for applications requiring high reliability in material performance in humid and external environments or underwater applications. Representative applications include coatings for electronic devices, materials for vehicles and aircraft, and structural water-resistant adhesives. However, it is important to note that common epoxies absorb a few to several wt % of water, and even this small amount of water severely affects their properties, such as glass transition temperature, elastic modulus, and adhesion. Against this background, numerous studies have been conducted to elucidate the details of water absorption,<sup>1,2</sup> as well as the relationship between the chemical structure of epoxy<sup>3,4</sup> and the underlying mechanism of water absorption and diffusion.<sup>5–7</sup> The structure of nanometer-scale voids (nanovoids) in resins<sup>8,9</sup> and the hydrogen bonding between water molecules and epoxy polymer chains<sup>10,11</sup> are widely recognized as key factors in the molecular diffusion mechanism of water in epoxy resins. However, the relationship among these factors and their relative importance has not yet been clarified. Furthermore, the possibility of additional

contributing factors highlights the complexity of water diffusion phenomena.

Molecular dynamics (MD) simulations are extensively employed as an effective tool for investigating water molecule dynamics in epoxy and its water-related phenomena. Research using MD simulations spans a wide range, including water penetration<sup>12–14</sup> and hydrolysis of epoxy polymers.<sup>15,16</sup> In recent years, the diffusion of water molecules in epoxy has been studied through water clustering within nanovoids and the relationship with hydrogen bonding, leading to a deeper understanding of the water diffusion mechanism based on void structures and polar interactions.<sup>17–19</sup> A characteristic hopping behavior of water molecules has been reported as a significant mode of water diffusion.<sup>13,17,19,20</sup> This hopping behavior is a widely observed phenomenon in simulations of the diffusion and transport of small molecules in various materials.<sup>21</sup>

**Received:** December 19, 2024

**Revised:** April 28, 2025

**Accepted:** April 29, 2025

However, voids are inherently discontinuous in epoxy; therefore, this behavior necessitates dynamic changes in void shape, and the mobility of the epoxy polymer chains surrounding the voids should be a crucial factor.<sup>5,7,17</sup> Despite this, compared to structural factors such as the void structure and hydrogen bonding, the relationship between the dynamics of epoxy polymer chains and the water diffusion mechanism remains largely unexplored.

The relationship between polymer chain mobility and small molecule diffusivity in thermoplastic polymers has been widely studied. Greater motion enhances diffusivity by influencing the structure of voids through which molecules move.<sup>21</sup> Since the segmental motion of polymer chains is correlated with the glass transition temperature ( $T_g$ ), a negative correlation between  $T_g$  and the diffusion coefficient has been experimentally demonstrated. On the other hand, our recent study on epoxies with different epoxide:amine stoichiometry revealed that the stoichiometric epoxy with an epoxide:amine ratio of 1:1 exhibited both a higher diffusion coefficient of water and a higher  $T_g$  compared to off-stoichiometric epoxies with excess epoxide or amine.<sup>22</sup> These results suggest that the relationship between the segmental motion of polymer chains and the diffusivity of small molecules, based on the studies of thermoplastic polymers, is not sufficient for epoxy, a typical thermosetting polymer. Instead, another aspect of polymer chain dynamics contributes significantly to the water diffusion mechanism in epoxy.

Furthermore, we investigated water molecule dynamics in epoxy on the picosecond time scale and nanometer spatial scale by quasi-elastic neutron scattering (QENS) measurements using water-sorbed deuterated epoxy.<sup>22</sup> The spatial dynamic behavior of water varied significantly depending on the epoxide:amine ratio of the epoxy system. Compared to off-stoichiometric epoxies, the stoichiometric epoxy exhibited a motion radius of water molecules more than four times larger, along with a higher proportion of highly mobile water molecules. Furthermore, additional QENS measurements of epoxy polymer chain local dynamics on a small unit or atomic scale using  $D_2O$ -absorbed nondeuterated epoxies revealed larger chain local dynamics in the stoichiometric epoxy compared to off-stoichiometric ones. These results indicated a correlation between water dynamics and the local mobility of the polymer chains, which is on a smaller scale compared to segmental motion.

Here, we conducted MD simulations on water-sorbed epoxy to elucidate the relationship among the composition ratio-dependent chemical structure of epoxy, the atomic mobility in polymer chains, and the water molecule dynamics. The local dynamic behavior of the polymer chains induces spatial changes in the voids within the epoxy. This change provides a mechanism to explain the diffusion of water molecules within epoxies via their characteristic hopping behavior and suggests that chain local mobility can serve as an effective indicator for understanding water diffusivity.

## SIMULATION METHODS

**General.** Full atomistic molecular dynamics simulations were performed with the large-scale atomic/molecular massively parallel simulator (LAMMPS) with the GPU package.<sup>23,24</sup> Winmostar V11 software was used for the pre- and post-treatments of the simulations. The atomic interactions were described by the GAFF force field, with atomic charges estimated from DFT calculations at the B3LYP/6–

31G(d,p) level of theory using the Gaussian 16 Rev. C.01 suite.<sup>25</sup> TIP3P was used for water molecules.<sup>26</sup> A time step of 1 fs was used for the NPT and NVT ensembles. The Nosé–Hoover thermostat and Parrinello–Rahman barostat were employed for temperature and pressure control.<sup>27</sup> A temperature changing rate of 1 K/ps and a pressure of 1 atm were used in all the NPT ensembles. Long-range electrostatic interactions were calculated by using the particle–particle mesh (PPPM) method with an accuracy of  $10^{-5}$ .<sup>28</sup> The simulation results were analyzed by OVITO software.<sup>29</sup>

**Preparation of Cross-Linked Epoxies.** The simulation cells before cross-linking contained a total of 600 molecules, consisting of bisphenol A diglycidyl ether (BADGE) and 4,4'-diaminodiphenylmethane (DDM) in predetermined ratios of 1:1 (300 molecules:300 molecules, EP1), 2:1 (400 molecules:200 molecules, EP2), and 3:1 (450 molecules:150 molecules, EP3). Initially, these molecules were randomly arranged to form an amorphous assembly with a density of 0.5 g/cm<sup>3</sup>. The simulation cell was relaxed at 800 K for 200 ps in the NVT ensemble, and then annealing–quenching steps were applied, including equilibration at 800 K for 100 ps, quenching to 453 K, equilibration at the same temperature for 350 ps, annealing to 800 K, and quenching to 453 K in the NPT ensemble. Then, it was equilibrated at this temperature for 3 ns in the NPT ensemble.

**Cross-Linking.** Cross-linking was performed using the bond/react package implemented in LAMMPS software.<sup>30,31</sup> The simulation was performed at 453 K, which is the temperature applied during the curing of epoxy samples in our previous experimental study.<sup>22</sup> Initially, the reaction between the epoxide and amine was carried out. The simulation time was set long enough (4 ns) to ensure the completion of the reaction or the plateau of its progress. Subsequently, the reaction between the remaining epoxide and hydroxyl groups was conducted in a similar manner. The cutoff distances for these reactions were set at 6 and 8 Å for epoxide–amine reactions and 8 Å for epoxide–hydroxyl reactions. The reaction probabilities were set at 0.04, 0.02, and 0.015, respectively. These parameters were determined by test simulations to ensure the consumption of the reactive groups without energetic failure, while also referring to previous studies.<sup>18,31</sup> After the cross-link reaction was performed, the resulting simulation cell was quenched to 338 K and then equilibrated at this temperature for 2 ns in the NPT ensemble. The deviations in the density of the obtained epoxy systems varied within 0.4% (EP2) to 8.2% (EP3), which indicated the practical reliability of these results.

**Preparation of Wet Epoxy.** Based on our previous experimental results, the number of water molecules to be added was 2.0 wt % of the epoxy weight for both EP2 and EP3.<sup>22</sup> Water molecules were randomly inserted into the simulation cell of epoxy at 338 K. The simulation cell underwent annealing to 800 K and then quenching to 333 K, equilibration at the same temperature for 350 ps, annealing from 800 K, and quenching to 333 K in the NPT ensemble. Then, it was equilibrated at the same temperature for 6 ns in the NPT ensemble.

**Diffusion Constant.** The diffusion coefficient of hydrogen atoms in water was calculated from the time dependence of the mean square displacement (MSD) of the hydrogen atoms using the following equation:

$$\text{MSD} = 1/N \cdot \sum_{i=1}^N \{ [R_i(t) - R_i(0)]^2 \}$$

where  $R_i(t)$  is the atom's coordinate at time  $t$ , and  $N$  is the number of atoms. The diffusion constant of each hydrogen atom was estimated by performing a linear regression on the time dependence of the MSD in a linear fitting.

**Void Analysis.** The void fraction in the hydrated epoxy was determined by using a probe with a radius of 1.4 Å on the epoxy matrix, from which water molecules were removed before the calculation.

**Atomic Displacement.** The displacement of polymer chain atoms was averaged over the entire simulation time (0–6 ns) using displacement values calculated for each 2 ps interval. All epoxy atoms, except for polar hydrogen atoms (O–H, N–H), were included in the calculations. The validity of this interval is discussed in the Discussion section. Additionally, to account for mobility changes due to neighboring atoms, average displacement values were also calculated from the displacements of adjacent atoms covalently bonded to the target atom (Supporting Information).

## RESULTS

**Simulation of Water Molecule Diffusion.** We conducted simulations on epoxies structurally identical to those studied through QENS measurements.<sup>22</sup> These epoxies are composed of bisphenol A diglycidyl ether and 4,4'-diaminodiphenylmethane with different stoichiometric ratios of 1:1 (EP1), 2:1 (EP2), and 3:1 (EP3) (Figure 1). While EP2 is a stoichiometric ratio, EP1 and EP3 are off-stoichiometric, with excess amine groups or excess epoxide groups. The QENS experiments utilized deuterated compounds and heavy water (D<sub>2</sub>O), whereas the simulations were conducted with compounds containing hydrogen atoms.

In the preparation of the cross-linked epoxy simulation cell, first, the reactions between NH<sub>2</sub> or NH and epoxide (N-link reaction) were performed. Then, the reactions between OH and epoxide (O-link reaction) were performed (Figure S1). This stepwise process is reasonable due to the significantly higher N-link reaction rate compared to the O-link reaction. More precisely, as the curing progresses, the collision frequency of the reaction sites becomes limited by geometric restrictions, altering the relative reaction rate. However, we adopted this simple stepwise process for the cross-linked epoxy network. In the subsequent O-link reaction, all epoxide groups were consumed in EP2, while a small amount of epoxide groups remained in EP3. Table S1 summarizes the number of cross-link points and the functional groups within the epoxy network structure. When counting the cross-links formed by both N and O reactions, the cross-link density follows the order EP2 < EP3. Water molecules were added to the resulting networks in accordance with experimentally determined equilibrated water absorption amounts to produce wet epoxies, wet-EP2 and wet-EP3 (Figure 2). The structural information on these systems is summarized in Table 1. Simulation for EP1 resulted in a significant amount of unreacted primary or secondary amine groups, yielding significantly varying cross-linked structures with each calculation. Consequently, information from wet-EP1 was strongly dependent on the initial network structure, and the effect of the less cross-linked network structure severely complicated the following discussion of cross-linked epoxies. Therefore, while we report

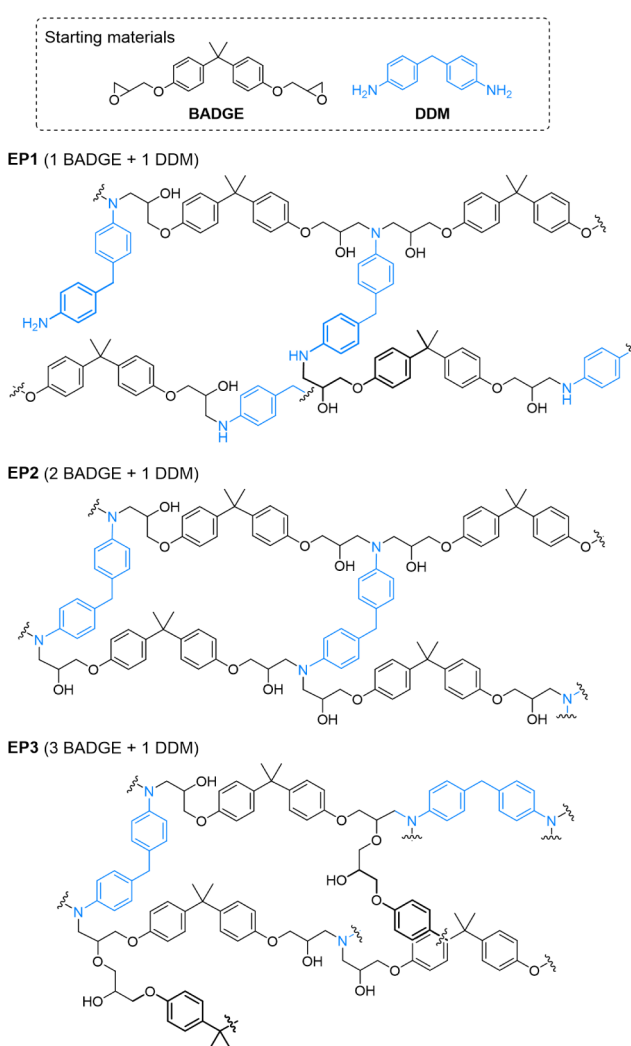


**Figure 1.** Chemical structure of epoxy in this work. The composition ratio of starting materials for EP2 is stoichiometric, while those for EP1 and EP3 are off-stoichiometric with excess amine and excess epoxide, respectively.

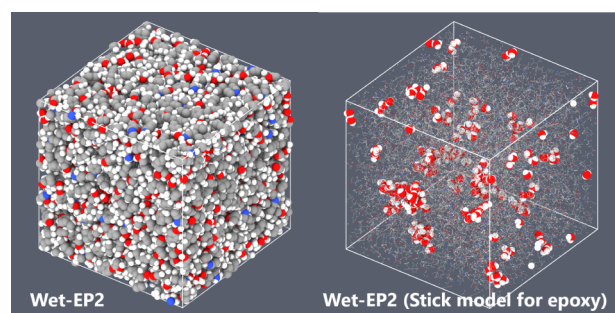


**Figure 2.** Structures of wet-EP2 represented using a space-filling model (left) and a space-filling model for water molecules inside and a stick model for the epoxy polymer (right).

preliminary results for wet-EP1 in the Supporting Information (Section 3 of SI), we have excluded wet-EP1 from subsequent experiments.

The apparent diffusion coefficients ( $D_{\text{eff}}$ ) of the hydrogen atom in water molecules were determined from the mean square displacement (MSD) of these atoms, and  $D_{\text{eff}}$  was larger in wet-EP2 than in wet-EP3 (Table S1 and Figure S2).

**Table 1. Epoxy Structure Information in These Simulations<sup>a</sup>**

Item	wet-EP2	wet-EP3
<b>Epoxy composition</b>		
BADGE	400	450
DDM	200	150
BADGE:DDM ratio	2:1	3:1
total number of atoms	25 400	26 400
number of water molecules	195	203
<b>Resulting epoxy structure</b>		
number of OH groups	720	600
water-accessible void fraction (%), average	7.2	7.8
density (g/mL)	1.10	1.11
deviation from the experimental sample (%) <sup>22</sup>	0.4	7.5

<sup>a</sup>For more detailed information, see Table S1.

Although the log–log plot of MSD showed the subdiffusion behavior of water molecules (Figure S3), the order of  $D_{\text{eff}}$  agrees with the diffusion coefficient obtained experimentally through bulk water absorption tests using Fick's law, as well as QENS experiments.<sup>22</sup> However, due to the inherent differences in each method, the  $D_{\text{eff}}$  values did not agree numerically. The experiment using Fick's law observes a nonequilibrium water absorption process, whereas QENS measurements and the presented MD simulations observe the dynamics of water molecules in equilibrium states. In addition, MD simulations derive  $D_{\text{eff}}$  from the movement of all water molecules, while QENS measurements specifically observe the dynamics of highly mobile water molecules and calculate  $D_{\text{eff}}$  by the adopted model.<sup>22,32</sup> Therefore, this study focused on the trends of water dynamics, that is, **wet-EP2** exhibits higher water molecule diffusivity compared to **wet-EP3**, and its underlying mechanisms.

Figure 3 illustrates the dynamic behavior of water molecules in **wet-EP2**, represented through the total displacement of hydrogen atoms in individual water molecules. Typical behaviors are represented by a hydrogen atom that shows long-range diffusion ( $H_a$ ) and those that showed minimal diffusion ( $H_b$  and  $H_c$ ). For convenience, we refer to these water molecules as  $H_2O_w$ , such as  $H_2O_a$ . The trajectory of  $H_a$  in water molecule  $H_2O_a$  with significant displacement, and the void in **wet-EP2** during the whole simulation period (0–6 ns) are shown in Figure 3b. Inherently, due to the densely cross-linked structure of epoxy, the chains are fixed in the same region, and the positions of voids are also essentially fixed. However, the shape of the void fluctuates. It is notable that while the voids related to the water molecule trajectory are not continuously interconnected throughout the entire simulation period, they exhibit interconnected structures at specific time instances. The plot of displacement exhibits three distinct behaviors: 1) *stay*: small displacement of less than 4–5 Å, as shown in the snapshot at 3100 ps. 2) *Hopping*: large displacement of more than 5–10 Å at a moment, as observed in the snapshots at 1380, 1382, and 1384 ps. In this behavior, water molecules quickly move between voids at the moment when voids are connected. 3) *Roaming*: consecutive moderate displacements, as shown in the snapshot at 700 ps. Since water molecules move over a wide range via repeated hopping, it is indicated that the formation and connectivity of transient voids play a crucial role in the water diffusion mechanism.

**Analysis of Bonding Interactions and Voids.** Before analyzing the dynamics of polymer chains and water molecules,

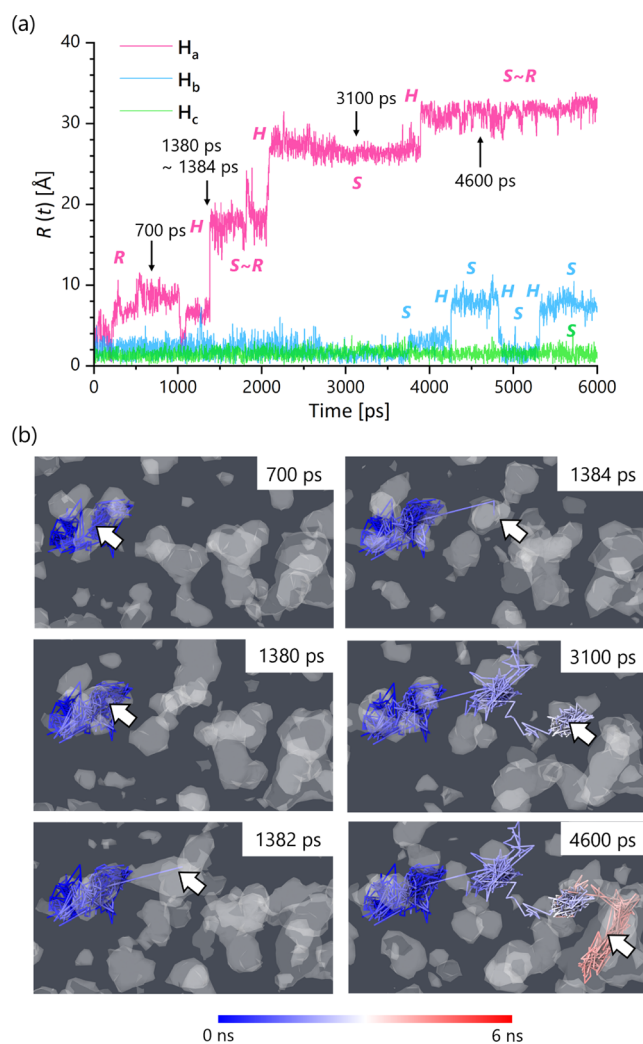


**Figure 3.** (a) Hopping-diffusion behavior of water molecules in **wet-EP2** monitored by hydrogen atoms every 2 ps, where  $R(t)$  is the displacement magnitude defined as  $R(t) = \{[r(t) - r(0)]^2\}^{0.5}$ , where  $r(t)$  and  $r(0)$  are the position of atoms at time  $t$  and 0 ps. Dynamic behaviors are categorized by their type:  $H$ , hopping;  $S$ , stay;  $R$ , roaming. Data are presented for three representative water molecules with different total displacement:  $H_a$  with long-range diffusion,  $H_b$  with limited diffusion, and  $H_c$  with virtually no movement. (b) Visualization of the trajectory (line) of  $H_a$  and the void in **wet-EP2** (white space). The trajectories are drawn from the initial positions up to the time point shown in each figure, and the white arrows indicate the positions of water molecules at that specific time. Color of the trajectory line represents the time point (color bar is shown in the bottom). The dark gray areas represent regions occupied by epoxy atoms.

we analyzed the structural characteristics of these epoxy systems with respect to hydrogen bonding interactions and voids. Radial distribution function (RDF) analysis of **wet-EP** demonstrated the presence of hydrogen bonding between water molecules and hydroxyl groups of the epoxy polymer (Figure 4). While **wet-EP3** showed a lower number of hydroxyl groups compared to **wet-EP2**, **wet-EP3** showed a greater propensity for hydrogen bond formation between water and hydroxyl groups. RDF analysis within the epoxy polymer suggests the existence of hydrogen bonding between hydroxyl groups and ether oxygen, forming a five-membered ring, and this tendency is more pronounced in **wet-EP2**. The formation

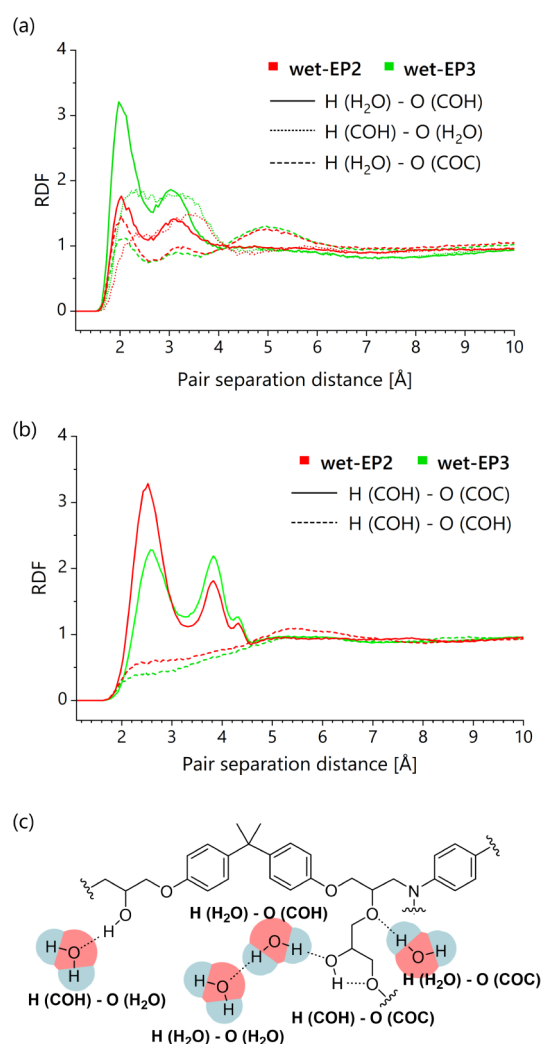


**Figure 4.** Radial distribution function (RDF) analysis of atoms in the **wet-EP2** and **wet-EP3** simulation cells. (a) Pair analysis between atoms in the epoxy polymer (oxygen or hydrogen atoms in alcohol (COH) or ether (COC) groups) and atoms in water molecules (hydrogen or oxygen atoms). The line color indicates **wet-EP2** or **wet-EP3**, and the line type indicates the pair. (b) Pair analysis between atoms in the epoxy polymer. (c) Chemical structure of the epoxy system with the O-link, showing proximity of atoms by dotted lines.

of the hydrogen bonding is apparently complementary to that between hydroxyl groups and water molecules. These results explain the lower water diffusivity in **wet-EP3** compared to **wet-EP2**.<sup>11,18,19,33</sup> The difference in the hydrogen bond formation between **wet-EP3** and **wet-EP2** is likely attributed to the presence of numerous O-links in **EP3**. The hydrogen bonding affects the steric environment around hydroxyl groups and disrupts the regular functional group sequence of hydroxyl groups and adjacent phenoxy alkyl ether groups. While these features indicate the confinement effect on water molecules in voids, they are insufficient to explain the hopping behavior.

Next, the effective void fraction with respect to water molecules was calculated, and **wet-EP2** and **wet-EP3** yielded nearly identical values as well as number of voids. It is noteworthy that the estimated radius of voids, based on the above analysis, showed good agreement with the radius experimentally determined using positron annihilation lifetime spectroscopy (PALS) in our previous work.<sup>22</sup> Information on

water cluster formation was provided by RDF analysis of oxygen–oxygen atom pairs between water molecules (Figure S4a).<sup>11,18</sup> The cluster size analysis showed that the existence of orphan water molecules is more pronounced in **wet-EP3** (Figure S4b). Conversely, **wet-EP2** showed a slightly higher tendency to form large clusters than **wet-EP3**. Although the reason for this difference is not yet fully clarified, it is possible that in **EP3**, the movement of water molecules through the interconnection of voids occurs less frequently compared to that in **EP2**, while in **EP2**, the presence of large voids formed by interconnection is more significant. Large cluster formation suggests the presence of large voids in which water molecules move in the *roaming* behavior. However, cluster formation is not directly related to the *hopping* behavior or overall transportation of water molecules, as indicated by the analysis of the average total displacement of water molecules belonging to clusters of different sizes (Figure S5).

To elucidate the mechanism underlying the hopping water dynamics, we analyzed the temporal variations in the void. For both **wet-EPs**, the void fraction and count remained constant over time (Figure S6). Moreover, a plot superimposing the time variation of voids and the displacement of highly mobile water showed virtually no correlation between hopping behavior and changes in the void fraction or void count (Figure S7). On the other hand, a notable change during the simulation was the temporal variation in void shape (Figure 5).

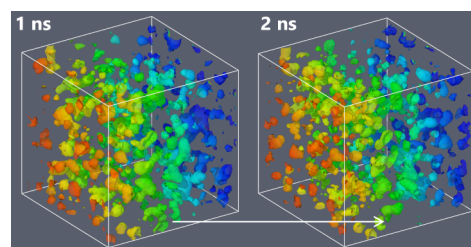


**Figure 5.** Water-accessible void distribution for **wet-EP2**. Two instantaneous moments at 1 and 2 ns of simulation time point are shown. The voids are shown without the water present in them, and their color represents the Y coordinate. One of the void changes is highlighted with a white arrow.

As previously mentioned, the hopping of water molecules occurs between transiently connected voids (Figure 3); therefore, it is essential to analyze these void shape changes induced by the polymer chain motion.

**Analysis of Chain Local Mobility.** To analyze the dynamics of polymer chains, we calculated the average atomic displacement of each atom in the chain over a short period to represent the local mobility of polymer chains (Figure 6). We employed the mobility of polymer chains at 2 ps as an indicator of atomic mobility ( $\Delta r_{2\text{ps}}$ ). The average displacement over the entire simulation time, represented by the MSD of polymer atoms, is widely used to analyze molecular mobility (Figure S2). However, it would not be the most appropriate metric for characterizing the hopping behavior and diffusion mechanism of water molecules because the geometric constraint on polymer chains may lead to an underestimation of atomic mobility. In contrast, chain motion within a short period is sufficient to form a transient interconnection of voids. From the analysis of water molecule displacement shown in Figure 3, the hopping movement of water through interconnected voids is an event completed in approximately

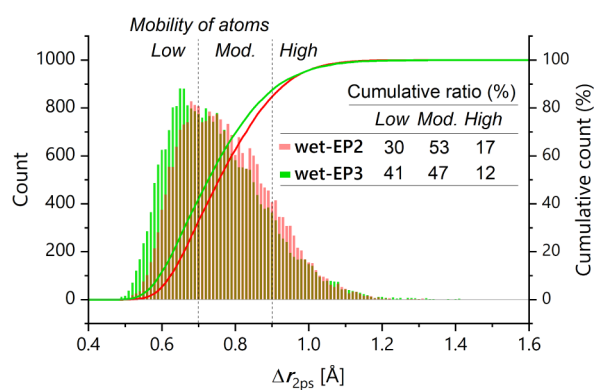


**Figure 6.** Histogram of the average atomic displacement ( $\Delta r_{2\text{ps}}$ ) of the polymer chains in **wet-EP2** and **wet-EP3**, and the cumulative count of atoms (in %). The inset table shows the proportion of atoms classified by the degree of mobility, low, moderate (Mod.), and high, which were defined according to a fixed numerical division of the distribution area.

2–4 ps. The optimization of the time interval for atomic mobility is important for the interpretation of the diffusion mechanism, which will be discussed further in the next section.

The distribution  $\Delta r_{2\text{ps}}$  for **wet-EP2** and **wet-EP3** was similar and distributed approximately from 0.5 to 1.3 Å. However, by analyzing the distribution bias as described below, it was found that the  $\Delta r_{2\text{ps}}$  distribution for **wet-EP2** is shifted toward higher mobility than **wet-EP3** (Figure 6). This indicated that the overall local mobility of the polymer in **wet-EP2** is greater than that in **wet-EP3**. These results align with our experimental observations of the comparison of polymer chain dynamics in **wet-EP2** and **wet-EP3** from QENS experiments using  $\text{D}_2\text{O}$ -absorbed epoxies.<sup>22</sup> To categorize atoms based on their mobility, this range was equally divided into four sections, each spanning 0.2 Å. Atoms belonging to the section with the smallest  $\Delta r_{2\text{ps}}$  ( $<0.7$  Å) were defined as having low mobility, those in the two sections with large  $\Delta r_{2\text{ps}}$  ( $\geq 0.9$  Å) were defined as having high mobility, and the rest were classified as having moderate mobility (Figure 6). Regarding the distribution of  $\Delta r_{2\text{ps}}$  in **wet-EP2**, the mean value, median, and peak value of the distribution were all larger compared to those in **wet-EP3** (Table S1). Notably, the most significant difference is the proportion of low-mobility atoms. Similar analytical conclusions were obtained from another analysis of atomic mobility defined by the average of neighboring atoms (Figure S8).

This analysis suggested that the expected void interconnection induced by epoxy chain dynamics is less likely to occur in EP3 than in EP2, depending on the chain atomic mobility, and vice versa. Figure 7 shows the trajectory of  $H_a$  of  $\text{H}_2\text{O}_a$  exhibiting significant total displacement with hopping behavior (Figure 3), voids at an instantaneous 2 ns snapshot, and polymer chain atoms with a color indicator showing each  $\Delta r_{2\text{ps}}$  value. This image shows that water preferentially moves within individual voids and the adjacent regions composed of chain atoms with large  $\Delta r_{2\text{ps}}$ , namely, regions of high local mobility, over a short period. The fact that these regions overlap with the trajectory indicates that void interconnection and formation occur at the sites where polymer chain local mobility is high. On the other hand, it is clearly illustrated that the low-mobility water molecule, without hopping behavior, is surrounded by chain atoms with low  $\Delta r_{2\text{ps}}$  (Figure S9). Thus, the atomic displacement over a short period,  $\Delta r_{2\text{ps}}$ , serves as a

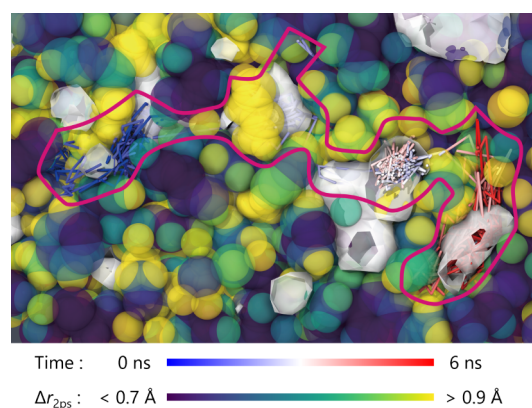


**Figure 7.** Trajectory line of  $H_a$  of water molecule  $\text{H}_2\text{O}_a$  exhibiting significant total displacement transporting between voids in **wet-EP2**. The trajectory is over a simulation duration of 6 ns with a slice of an epoxy chain and a void structure. Color of the trajectory line (blue-to-red colored line) represents the time point. White spaces are voids, and the spheres are epoxy polymer chain atoms. The color of epoxy atoms indicates each  $\Delta r_{2\text{ps}}$ . The purple line was used to indicate the outer edge of the region where the water trajectory exists because most of the trajectory is hidden by the atoms.

metric for water molecule hopping behavior and is useful for evaluation of relative water molecule diffusivity, because sufficient chain atom local mobility is requisite for the void interconnection necessary for hopping behavior (Figure 8).

Comparison of different moieties within each epoxy consistently found higher atomic mobility in alkyl moieties than in aryl moieties (Figure 9a,b). This result agrees with the fact that atoms in alkyl moieties exhibit higher freedom and flexibility due to the rotational motion around single bonds. These results suggest that alkyl moieties contribute more than aryl moieties to the interconnection of voids through local dynamics. **Wet-EP2** exhibited higher  $\Delta r_{2\text{ps}}$  in both alkyl and aryl moieties compared to **wet-EP3** (Figure 9c,d). The critical structural difference between EP2 and EP3, namely the O-link, is involved in the alkyl chain; however, it causes a decrease in local mobility across the entire polymer network regardless of the chemical structural moiety. This observation suggests that experimental determination of atomic mobility in either the alkyl, aryl, or a subset thereof could be used to compare the entire network mobility of different epoxies.

## DISCUSSION

Compared to water transport phenomena within porous materials such as zeolites<sup>20</sup> and metal–organic frameworks (MOFs),<sup>34</sup> diffusion within densely cross-linked polymers such as epoxy resins exhibits markedly different characteristics. This arises because voids in epoxy resins are irregular and discontinuous, providing no apparent pathways for the transport of water molecules (Figures 3, 5, and 7). The disconnected void structure significantly restricts the mobility of the water molecules confined within each void. Long-distance diffusion of water molecules via intervoid hopping behavior requires transient void connections arising from polymer chain motion (Figure 3). Furthermore, the relationship between polymer chains and voids in epoxy differs from that in thermoplastic polymers.<sup>21</sup> In thermoplastic polymers, the segmental motion of polymer chains plays a more crucial role than local motion in the mechanism of void structure changes related to water diffusion. In epoxy, a thermosetting

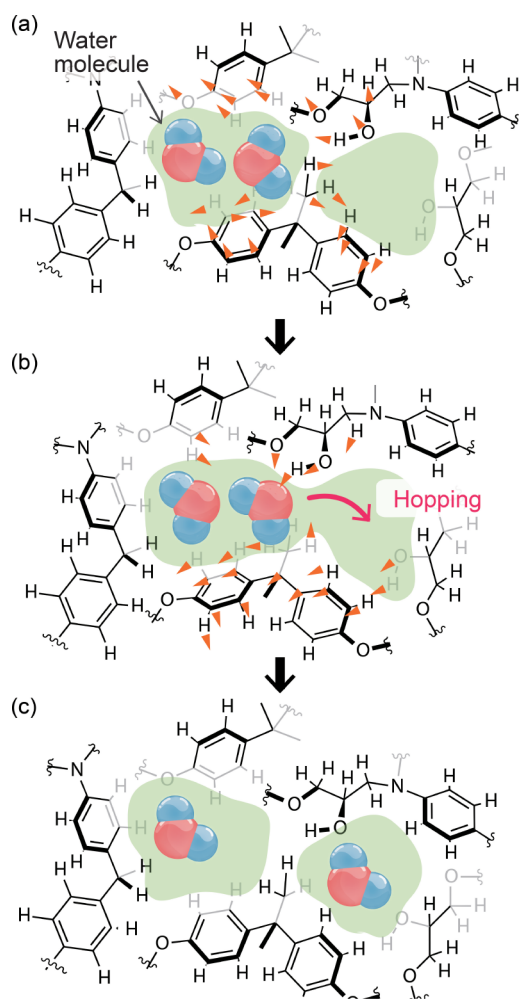


**Figure 8.** Schematic illustration of the proposed method for water molecule dynamics in relation to epoxy atomic displacement. The green region indicates voids in the epoxy, and the orange triangles indicate the atomic displacement for the next conformation. (a, c) Individual voids separated by the epoxy atoms, and (b) temporarily interconnected voids owing to the dynamic motion (atomic displacement) of epoxy. Some atomic displacement (orange arrow) are omitted for clarity.

polymer, the polymer chains are constrained by the densely cross-linked structure, preventing large-scale segmental movement. Therefore, chain local motion becomes significant in epoxies.

Regarding the dynamics of water molecules in voids, the confinement effect of hydrogen bonding between water and polar groups of the epoxy polymer was proposed.<sup>18,19</sup> In our results, **wet-EP3**, which exhibited lower water diffusivity, showed a higher probability of hydrogen bonding between water and the polymer in RDF analysis compared to **wet-EP2** (Figure 4), supporting this proposition. The frequency of water molecule hopping events is determined by void interconnection induced by high polymer chain mobility. These results suggest that hydrogen bonding and chain local mobility are distinct factors for confinement within voids and hopping behavior, respectively, and that the water diffusion mechanism is a combination of these factors. The analysis of the number of hydrogen bonds between water molecules and the polar sites of the polymer chain suggested that the number of hydrogen

bonds is not necessarily associated with hopping behavior (Figure S10).

The chain local mobility represented by  $\Delta r_{2\text{ ps}}$  demonstrated a correlation between highly mobile chain atoms and void interconnection (Figure 7). The observation that epoxy resins with a higher proportion of mobile polymer chain atoms showed enhanced water diffusion corroborates this relationship (Figure 6). These results validated the utility of  $\Delta r_{2\text{ ps}}$  as a metric for evaluating the hopping behavior of water molecules between different epoxies. A recently reported study approached the relationship between chain mobility and water diffusivity using the bond rotational energy barrier of monomers constituting epoxy chains as a metric, and it demonstrated that structures with lower barrier energies exhibited higher calculated diffusion coefficients.<sup>17</sup> Because chain atomic displacement  $\Delta r_{2\text{ ps}}$  is attributed to conformational changes via rotation around covalent bonds,  $\Delta r_{2\text{ ps}}$  and the rotational energy barrier appear to provide similar information regarding polymer chain mobility. However, given that epoxy possesses a dense molecular structure, its mobility is significantly influenced by the molecular packing and the local environment, even for chemically identical structural sites. Consequently,  $\Delta r_{2\text{ ps}}$  and the rotational energy barrier convey distinct information in mechanistic analysis, providing the spatial and temporal degree of atomic mobility and an energetic parameter, respectively.

The optimal time interval for defining polymer chain atomic displacement  $\Delta r$  remains open to debate, as it should theoretically correspond to the characteristic time scale of hopping behavior. However, our additional investigations demonstrated that variations in the time interval for calculating atomic displacement (1–10 ps, Figure S11) yielded distributions similar to those obtained using 2 ps ( $\Delta r_{2\text{ ps}}$ , Figure 6), while maintaining consistent differences between **wet-EP2** and **wet-EP3**. Therefore, the present analysis proved sufficient to elucidate the relationship between water molecule diffusion and polymer chain atomic mobility.

For a reliable model of water molecule diffusion, it is essential to develop a deeper understanding of the chemical factors influencing diffusion in polymer networks. We have demonstrated that the small-scale local motion of polymer chains plays a crucial role in water diffusion behavior in densely cross-linked networks, such as epoxy resins. The widely accepted physical model of diffusion includes parameters representing chemical interactions or structural factors.<sup>21</sup> The factor that we proposed will contribute to a more accurate description of the diffusion process through these parameters. While the atomic displacement  $\Delta r$  allows for a relative comparison between different epoxy systems, further considerations, such as parametrizing void connectivity and molecular hopping frequency, are necessary to incorporate local chain mobility into the diffusion model.

## CONCLUSION

We conducted molecular dynamics simulations to investigate the dynamics of internal water molecules in two epoxies with different composition ratios. In epoxy, the polymer chains are structurally constrained by dense cross-linking, and large-scale segmental motion of polymer chains is restricted. Therefore, the importance of small-scale chain local mobility in the diffusion process is more significant in epoxy than in thermoplastics. The analysis of epoxy polymer chain local mobility provided an explanation for the discontinuous

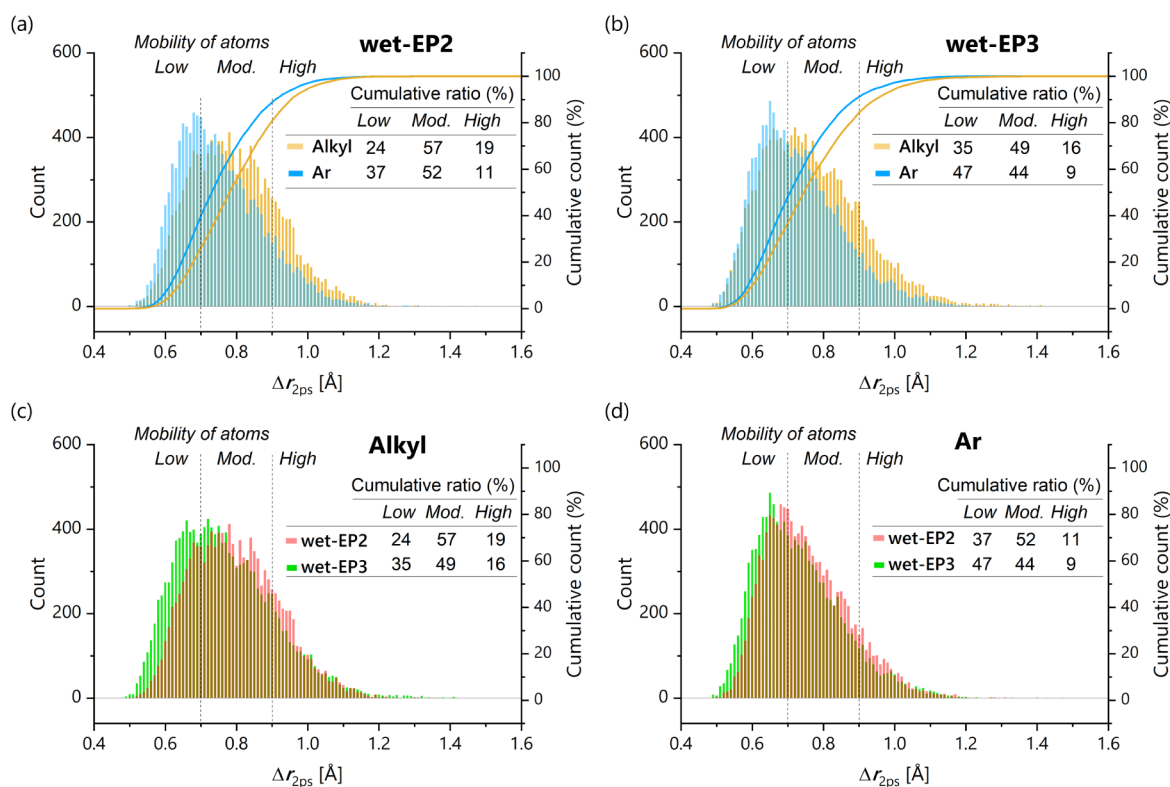


**Figure 9.** Distribution of polymer chain atomic mobility comparing the chemical structure moiety. Comparison of the alkyl and aryl moieties in wet-EP2 (a) and wet-EP3 (b), respectively. Comparison of wet-EP2 and wet-EP3 for alkyl (c) and aryl (d) moieties, respectively.

diffusion phenomena of water, encompassing both confinement in a void and hopping behavior. This discontinuous diffusion cannot be adequately explained solely by conventional structural factors, such as void size and water–polymer hydrogen bonding. Polymer chain local mobility and the two aforementioned factors are intricately involved in different aspects of the water diffusion mechanism: void size defines the constraint space for water molecules and cluster formation, hydrogen bonding affects the confinement within a void, and chain mobility facilitates hopping behavior.

The chain local mobility is contingent upon geometric and chemical structure factors, such as cross-link density and intra- or intermolecular hydrogen bonding of hydroxyl groups in epoxy. Therefore, a comprehensive understanding of the water diffusion mechanism still necessitates an integrated analysis of both molecular and nanostructural characteristics from both structural and dynamic perspectives. This work suggests that water diffusivity in cross-linked resins can be understood and controlled through the small-scale, atomic local mobility of polymer chains. Such analysis and design approaches will contribute to a deeper understanding of water-related properties in epoxy materials and facilitate material optimization.

## ■ ASSOCIATED CONTENT

### SI Supporting Information

The Supporting Information is available free of charge at <https://pubs.acs.org/doi/10.1021/acsapm.4c04089>.

Additional table on the simulation information and related data, additional figures for simulation results, and the study on EP1 (PDF)

## ■ AUTHOR INFORMATION

### Corresponding Author

Yasuyuki Nakamura – Research Center for Macromolecules and Biomaterials, National Institute for Materials Science (NIMS), Tsukuba, Ibaraki 305-0047, Japan; [orcid.org/0000-0003-0078-6413](https://orcid.org/0000-0003-0078-6413); Email: [NAKAMURA.Yasuyuki@nims.go.jp](mailto:NAKAMURA.Yasuyuki@nims.go.jp)

### Authors

Yuji Higuchi – Research Institute for Information Technology, Kyushu University, Fukuoka, Fukuoka 819-0395, Japan; [orcid.org/0000-0001-8759-3168](https://orcid.org/0000-0001-8759-3168)

Yoshihisa Fujii – Department of Chemistry for Materials, Graduate School of Engineering, Mie University, Tsu, Mie 514-8507, Japan; [orcid.org/0000-0001-9419-8537](https://orcid.org/0000-0001-9419-8537)

Masanobu Naito – Research Center for Macromolecules and Biomaterials, National Institute for Materials Science (NIMS), Tsukuba, Ibaraki 305-0047, Japan; [orcid.org/0000-0001-7198-819X](https://orcid.org/0000-0001-7198-819X)

Complete contact information is available at: <https://pubs.acs.org/doi/10.1021/acsapm.4c04089>

### Notes

The authors declare no competing financial interest.

## ■ ACKNOWLEDGMENTS

This study was partially supported by the Japan Society for the Promotion of Science KAKENHI Grant No. 23K04845 (Y.N.), JP19H05718 (Y.H.), and JP19H05720 (Y.F.), and the Acquisition, Technology, and Logistics Agency (Japan) (Y.N.). Y.N. thanks Dr. T. Tominaga of the Neutron Science and Technology Center, Comprehensive Research Organiza-

tion for Science and Society (CROSS, Japan), for valuable discussions. Y.F. thanks National Institute for Materials Science (NIMS) Joint Research Hub Program.

## REFERENCES

- (1) Frank, K.; Wiggins, J. Effect of Stoichiometry and Cure Prescription on Fluid Ingress in Epoxy Networks. *J. Appl. Polym. Sci.* **2013**, *130*, 264–276.
- (2) De'Nève, B.; Shanahan, M. E. R. Water Absorption by an Epoxy Resin and Its Effect on the Mechanical Properties and Infra-Red Spectra. *Polymer* **1993**, *34*, 5099–5105.
- (3) Nakamura, Y.; Hibi, Y.; Naito, K.; Yamamoto, N.; Hanamura, M. Chemical Structure Evaluations of Amine Hardeners to Ensure and Predict the Performance of Wet Adhesion of Epoxies. *Bull. Chem. Soc. Jpn.* **2023**, *96*, 1339–1345.
- (4) Knox, S. T.; Wright, A.; Cameron, C.; Fairclough, J. P. A. Structural Variation and Chemical Performance—A Study of the Effects of Chemical Structure upon Epoxy Network Chemical Performance. *ACS Appl. Polym. Mater.* **2021**, *3*, 3438–3445.
- (5) Geise, G. M.; Paul, D. R.; Freeman, B. D. Fundamental Water and Salt Transport Properties of Polymeric Materials. *Prog. Polym. Sci.* **2014**, *39*, 1–42.
- (6) Wijmans, J. G.; Baker, R. W. The Solution-Diffusion Model: A Review. *J. Membr. Sci.* **1995**, *107*, 1–21.
- (7) Freeman, B. D. Basis of Permeability/Selectivity Tradeoff Relations in Polymeric Gas Separation Membranes. *Macromolecules* **1999**, *32*, 375–380.
- (8) Soles, C. L.; Chang, F. T.; Bolan, B. A.; Hristov, H. A.; Gidley, D. W.; Yee, A. F. Contributions of the Nanovoid Structure to the Moisture Absorption Properties of Epoxy Resins. *J. Polym. Sci. Part B: Polym. Phys.* **1998**, *36*, 3035–3048.
- (9) Soles, C. L.; Chang, F. T.; Gidley, D. W.; Yee, A. F. Contributions of the Nanovoid Structure to the Kinetics of Moisture Transport in Epoxy Resins. *J. Polym. Sci., Part B: Polym. Phys.* **2000**, *38* (5), 776–791.
- (10) Li, L.; Yu, Y.; Wu, Q.; Zhan, G.; Li, S. Effect of Chemical Structure on the Water Sorption of Amine-Cured Epoxy Resins. *Corros. Sci.* **2009**, *51*, 3000–3006.
- (11) Mijović, J.; Zhang, H. Local Dynamics and Molecular Origin of Polymer Network–Water Interactions as Studied by Broadband Dielectric Relaxation Spectroscopy, FTIR, and Molecular Simulations. *Macromolecules* **2003**, *36*, 1279–1288.
- (12) Tam, L.; Lau, D. Moisture Effect on the Mechanical and Interfacial Properties of Epoxy-Bonded Material System: An Atomistic and Experimental Investigation. *Polymer* **2015**, *57*, 132–142.
- (13) Pandiyan, S.; Krajniak, J.; Samaey, G.; Roose, D.; Nies, E. A Molecular Dynamics Study of Water Transport inside an Epoxy Polymer Matrix. *Comput. Mater. Sci.* **2015**, *106*, 29–37.
- (14) Zhang, D.; Li, K.; Li, Y.; Sun, H.; Cheng, J.; Zhang, J. Characteristics of Water Absorption in Amine-Cured Epoxy Networks: A Molecular Simulation and Experimental Study. *Soft Matter* **2018**, *14*, 8740–8749.
- (15) Karuth, A.; Alesadi, A.; Vashisth, A.; Xia, W.; Rasulev, B. Reactive Molecular Dynamics Study of Hygrothermal Degradation of Crosslinked Epoxy Polymers. *ACS Appl. Polym. Mater.* **2022**, *4*, 4411–4423.
- (16) Ogata, S.; Uranagase, M. Protonation of Strained Epoxy Resin under Wet Conditions via First-Principles Calculations Using the H<sup>+</sup>-Shift Method. *J. Phys. Chem. B* **2023**, *127*, 2629–2638.
- (17) Liu, Y.; Lin, Y.; Zhang, Y.; Cao, B.; Wu, K.; Wang, L. Understanding Water Diffusion Behaviors in Epoxy Resin through Molecular Simulations and Experiments. *Langmuir* **2024**, *40*, 4871–4880.
- (18) Yamamoto, S.; Kuwahara, R.; Tanaka, K. Dynamic Behaviour of Water Molecules in Heterogeneous Free Space Formed in an Epoxy Resin. *Soft Matter* **2021**, *17*, 6073–6080.
- (19) Vuković, F.; Walsh, T. R. Moisture Ingress at the Molecular Scale in Hygrothermal Aging of Fiber–Epoxy Interfaces. *ACS Appl. Mater. Interfaces* **2020**, *12*, 55278–55289.
- (20) Ohkubo, T.; Gin, S.; Collin, M.; Iwade, Y. Molecular Dynamics Simulation of Water Confinement in Disordered Aluminosilicate Subnanopores. *Sci. Rep.* **2018**, *8* (1), 3761.
- (21) *Materials Science of Membranes*, Yampolskii, Y.; Pinnau, I.; Freeman, B., Eds.; John Wiley & Sons, Ltd, 2006.
- (22) Nakamura, Y.; Tominaga, T.; Iwata, T.; Inoue, K.; Fujii, Y.; Oshima, N.; Naito, M. Spatial Dynamics of Water Molecules Confined in Deuterated Epoxies by Quasi-Elastic Neutron Scattering. *Macromolecules* **2024**, *57*, 4254–4262.
- (23) Thompson, A. P.; Aktulga, H. M.; Berger, R.; Bolintineanu, D. S.; Brown, W. M.; Crozier, P. S.; in't Veld, P. J.; Kohlmeyer, A.; Moore, S. G.; Nguyen, T. D. LAMMPS - a Flexible Simulation Tool for Particle-Based Materials Modeling at the Atomic, Meso, and Continuum Scales. *Comput. Phys. Commun.* **2022**, *271*, 108171.
- (24) Brown, W. M.; Wang, P.; Plimpton, S. J.; Tharrington, A. N. Implementing Molecular Dynamics on Hybrid High Performance Computers – Short Range Forces. *Comput. Phys. Commun.* **2011**, *182*, 898–911.
- (25) Frisch, M. J., et al. *Gaussian 16, Revision C.01*; Gaussian Inc.: Wallingford, CT, 2016.
- (26) Mark, P.; Nilsson, L. Structure and Dynamics of the TIP3P, SPC, and SPC/E Water Models at 298 K. *J. Phys. Chem. A* **2001**, *105*, 9954–9960.
- (27) Parrinello, M.; Rahman, A. Polymorphic Transitions in Single Crystals: A New Molecular Dynamics Method. *J. Appl. Phys.* **1981**, *52*, 7182–7190.
- (28) Hockney, R. W.; Eastwood, J. W. *Computer Simulation Using Particles*; Adam Hilger: New York, 1988.
- (29) Stukowski, A. Visualization and Analysis of Atomistic Simulation Data with OVITO—the Open Visualization Tool. *Modelling Simul. Mater. Sci. Eng.* **2010**, *18*, 015012.
- (30) Gissinger, J. R.; Jensen, B. D.; Wise, K. E. Modeling Chemical Reactions in Classical Molecular Dynamics Simulations. *Polymer* **2017**, *128*, 211–217.
- (31) Gissinger, J. R.; Jensen, B. D.; Wise, K. E. REACTER: A Heuristic Method for Reactive Molecular Dynamics. *Macromolecules* **2020**, *53*, 9953–9961.
- (32) Shudo, Y.; Izumi, A.; Hagita, K.; Yamada, T.; Shibata, K.; Shibayama, M. Diffusion Behavior of Methanol Molecules Confined in Cross-Linked Phenolic Resins Studied Using Neutron Scattering and Molecular Dynamics Simulations. *Macromolecules* **2018**, *51*, 6334–6343.
- (33) Popineau, S.; Rondeau-Mouro, C.; Sulpice-Gaillet, C.; Shanahan, M. E. R. Free/Bound Water Absorption in an Epoxy Adhesive. *Polymer* **2005**, *46*, 10733–10740.
- (34) Zhang, C.; Wu, B.-H.; Ma, M.-Q.; Wang, Z.; Xu, Z.-K. Ultrathin Metal/Covalent–Organic Framework Membranes towards Ultimate Separation. *Chem. Soc. Rev.* **2019**, *48*, 3811–3841.